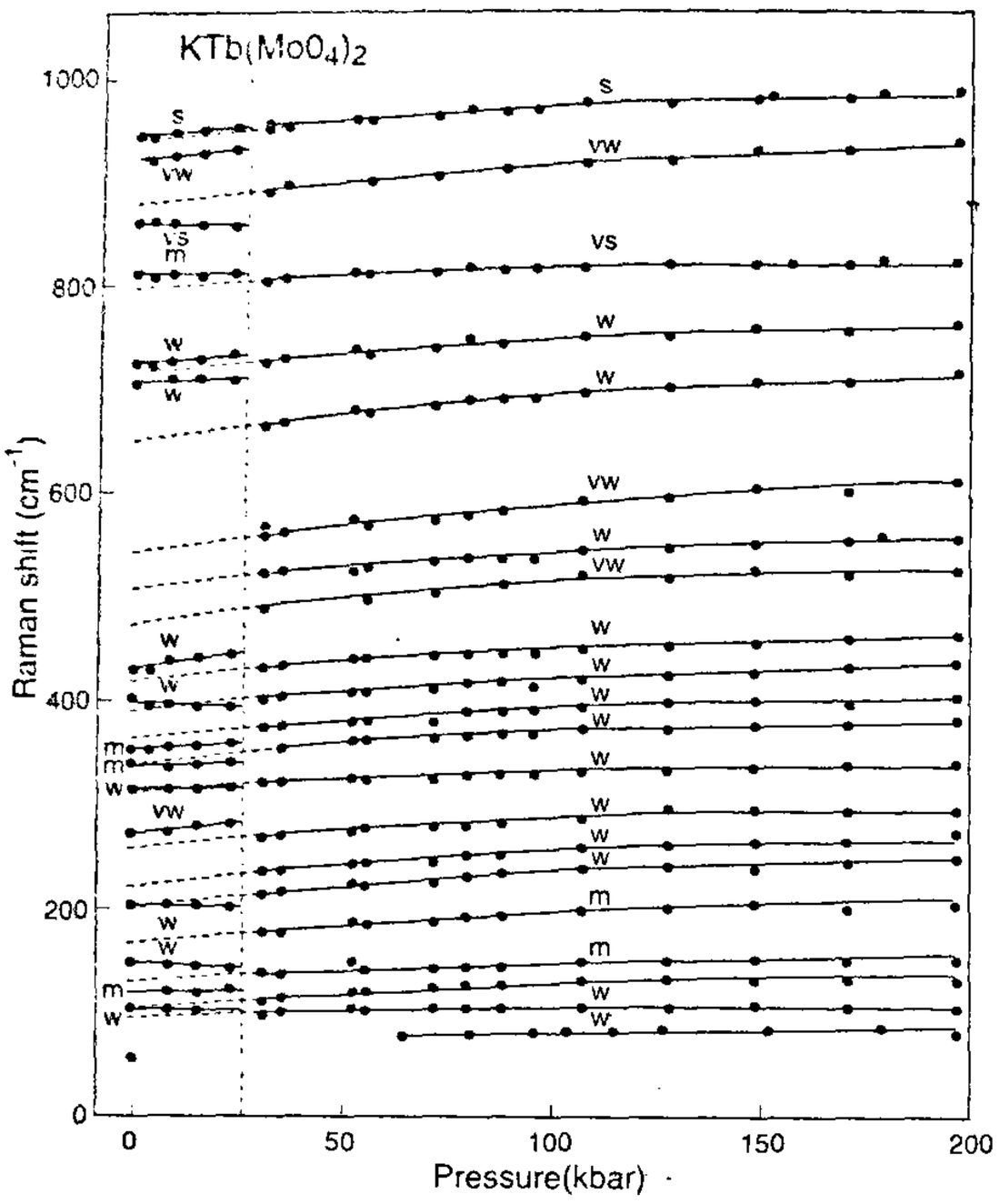


**Figure 3.** A plot of the observed Raman peak frequencies as a function of pressure. The vertical dotted line demarcates the phase transition pressure.

We believe that this is due to a charge transfer absorption (4f–5d) arising from a change in the valence state of Tb from $3^+$ to the $4^+$ state. The fact that Tb can exist in both the valence states is well known. The material after the phase transition is still an insulator, which means that the overall charge neutrality should be preserved. The way the charge compensation can happen is that the valence state of Mo becomes $Mo^{5+}$ from $Mo^{6+}$. This would then be a case of intervalence charge transfer between Tb and Mo from $Tb^{3+}Mo^{6+} \rightarrow Tb^{4+}Mo^{5+}$ similar to the case of $TlReO_4$ (ref. 7). Our picture for KTMO is that at the structural transition near 27 kbars the oxygens surrounding the Tb ion move closer to the terbium, causing an abrupt increase in the crystal field splitting of the 5d state of terbium. This brings down the 5d energy, facilitating 4f–5d transfer. To preserve charge neutrality the Mo readjusts its valence by the flow of electrons through the ligand. In the case of Y and Dy compounds, a valence change is not possible, and hence no colour change is observed, although an identical pressure-induced structural transition takes place in them. Thus, it is the structural transition that drives the charge transfer transition in KTMO and not the other way.

1. Trunov, V. K., Fremov, V. A. and Velikodnyi, Yu. A., *The Crystal Chemistry and Properties of Double Molybdates and Tungstates*, in Russian, Nauka, Leningrad, 1986.
2. Klevtzova, R. F. and Borisov, S. V., *Dok. Akad. Nauk. SSSR*, 1967, **177**, 1333–1336.
3. Jayaraman, A., Sharma, S. K., Wang, Z., Wang, S. Y., Ming, L. C. and Manghnani, M. H., *J. Phys. Chem. Solids*, 1993, **54**, 827–833.
4. Jayaraman, A., Wang, S. Y. and Sharma, S. K., *Solid State Commun.*, 1995, **93**, 885–888.
5. Hanuza, J. and Labuda, L., *J. Raman Spectrosc.*, 1981, **11**, 231–237.
6. Sokolovskii, B. M., Evdokimova, A. A. and Trunov, V. K., *Russ. J. Inorg. Chem.*, 1977, **22**, 816–819.
7. Jayaraman, A., Kourouklis, G. A. and Van Uitert, L. G., *Phys. Rev.*, 1987, **B36**, 8547–8551.

ACKNOWLEDGEMENTS. This work was supported by the Division of Materials Research of the National Science Foundation grant DMR-94-02443. We thank L. C. Ming and S. R. Shieh for the participation in the high pressure X-ray diffraction studies and for their permission to quote the results here.

Received 1 December 1995; accepted 29 December 1995

# Observation of negative remanence in an organic ferromagnet

**S. A. Chavan, J. V. Yakhmi, R. Ganguly and V. K. Jain**

Chemistry Division, Bhabha Atomic Research Centre, Trombay, Bombay 400 085, India

**DC magnetization measurements on two related ferromagnets, $(NBu_4)_2Mn_2[Cu(opba)]_3 \cdot 6DMSO \cdot H_2O$ ($T_c$ = 15 K) and $(NBu_4)_2Mn_2[Cu(opba)]_3$ ($T_c$ = 22 K) reveal the unusual phenomenon of negative remanent magnetization.**

THE occurrence of spontaneous magnetization in molecular organic materials was first reported in 1986 (ref. 1). Since then different categories of molecular ferromagnets have been synthesized depending on whether the unpaired electrons reside (i) in p orbitals only; (ii) in both p and d orbitals; and (iii) in d orbitals only. Kahn's group has synthesized a number of organic ferromagnets belonging to the last category by arranging ordered Q1D ferrimagnetic bimetallic chains in a bulk lattice in such a way to achieve a net ferromagnetic alignment of spins[2–4]. A typical example of such a bimetallic chain is $Mn^{II}Cu^{II}(obbz) \cdot nH_2O$ [obbz = oxamido bis(benzoato)] with an antiferromagnetic interaction between the adjacent local spins $S_{Mn} = 5/2$ and $S_{Cu} = 1/2$ separated by oxamido and carboxylato bridging groups which transmit the magnetic effects. When assembled appropriately in a 3D lattice, interchain interactions provide ferromagnetic order below 14 K for

$MnCu(obbz) \cdot 1H_2O$ (ref. 4). Recently, this group has reported Curie temperatures up to 22.5 K by increasing the dimensionality of the building blocks from chains to $MN^{II}_2Cu^{II}_3$ planar units in the new series of compounds $(cat)_2Mn_2[Cu(opba)]_3 \cdot S$, where $cat^+$ is a monovalent cation, opba is *ortho*-phenylenebis(oxamato) and S stands for solvent molecule[5]. All these $(cat)_2Mn_2[Cu(opba)]_3 \cdot S$ compounds are soft magnets with M(H) curves exhibiting very narrow hysteresis loops, with coercive field of 10 Oe or lower at 4.2 K. We have synthesized the compound $(NBu_4)_2Mn_2[Cu(opba)]_3 \cdot 6DMSO \cdot 1H_2O$, and the related desolvated compound $(NBu)_2Mn_2[Cu(opba)]_3$, hereafter called **A** and **B** respectively, for which $T_c$-values have been reported to be 15 K and 22 K by Stumpf *et al.*[6]. Our dc magnetization studies indicate negative thermo-remanent magnetization behaviour for both of these compounds, a novel phenomenon observed for the first time for organic ferromagnets, brief details of which are given in this paper. Negative remanence had, of course, been reported in the literature for cobalt vanadate, a ferrimagnet[7].

The sample **A** was synthesized following the procedure given by Stumpf *et al.*[6]. A portion of the sample **A** was heated at 175°C for about three hours under vacuum to remove the solvent molecules $6DMSO \cdot 1H_2O$ and was called **B**. AC susceptibility measurements were made on these two samples using an A.P.D. susceptometer with EG & G Model 5208 Lock-in Amplifier exhibited a sudden divergence at 16 K and 22 K, respectively, in agreement with the reported Curie temperatures. DC magnetization measurements were taken using EG & G.P.A.R. Model 4500 Vibrating Sample Magnetometer fitted with a Walker electromagnet and Tidewater bipolar power supply both as a function of temperature, $M(T)$ and applied field, $M(H)$. A Hall-probe guassmeter was used to check the absence of residual field between the poles down to < 1 Oe.

Zero field-cooled magnetization (ZFCM) data were recorded by cooling the sample down to 5 K in zero applied field, switching on the applied field (10 Oe) at this temperature and recording the magnetization while warming the sample up. Field-cooled magnetization (FCM) data were collected after cooling the sample in 10 Oe field and recording the data while warming up, keeping the field on. Remanent magnetization (REM) data were collected after cooling the sample to 5 K under an applied field of 10 Oe (or higher fields, as required), and recording the data while warming up, after reducing the field to zero.

Figure 1 shows the ZFCM, FCM and REM data as a function of temperature for the sample **B**, weighing 42.8 mg. The literature on different ferromagnetic materials reports positive values of magnetization for all these three parameters. Hence, as per convention, the scale chosen for this sample was 0 to + 900 memu/g to suit the FCM data which should normally have the higher magnitude among the three parameters. However, the remanence value which was about + 50 memu/g at 5 K, dropped sharply upon warming, becoming zero at 11.5 K and attained negative values between 11.5 K and 20 K, becoming positive again for temperatures above 20 K. The complete REM plot for the sample **B** was therefore recorded again under appropriate scales as shown in Figure 2. The ZFCM curve for ferromagnets, including those belonging to the category of bimetallic organic ferromagnets reported thus far, always lies much lower than the FCM because the domain walls do not move freely. However, ZFCM plot for the sample **B** is only marginally lower than the FCM in the range of temperature, $5 K < T < 13 K$ and both ZFCM and FCM nearly overlap for $T > 13$ K and even criss-cross a number of times (Figure 1), which is quite rare and implies that the domain walls are able to move rather freely. The observation of negative remanence is novel and intriguing. One obvious question that comes to mind is, whether negative remanence was caused by any residual negative field present between the pole pieces of the electromagnet. We have checked that the residual field before making any measurements is less than 1 Oe (plus or minus). Nonetheless, in order to give further credibility to our data, we also present in Figure 2 the REM data taken on a standard Ni sample and another organic ferromagnet $MnCu(obbz) \cdot 1H_2O$ ($T_c = 14$ K) that show positive values of REM, as expected. The remanence for the sample **B** continued to exhibit negative values and valley-like shape even at higher values of

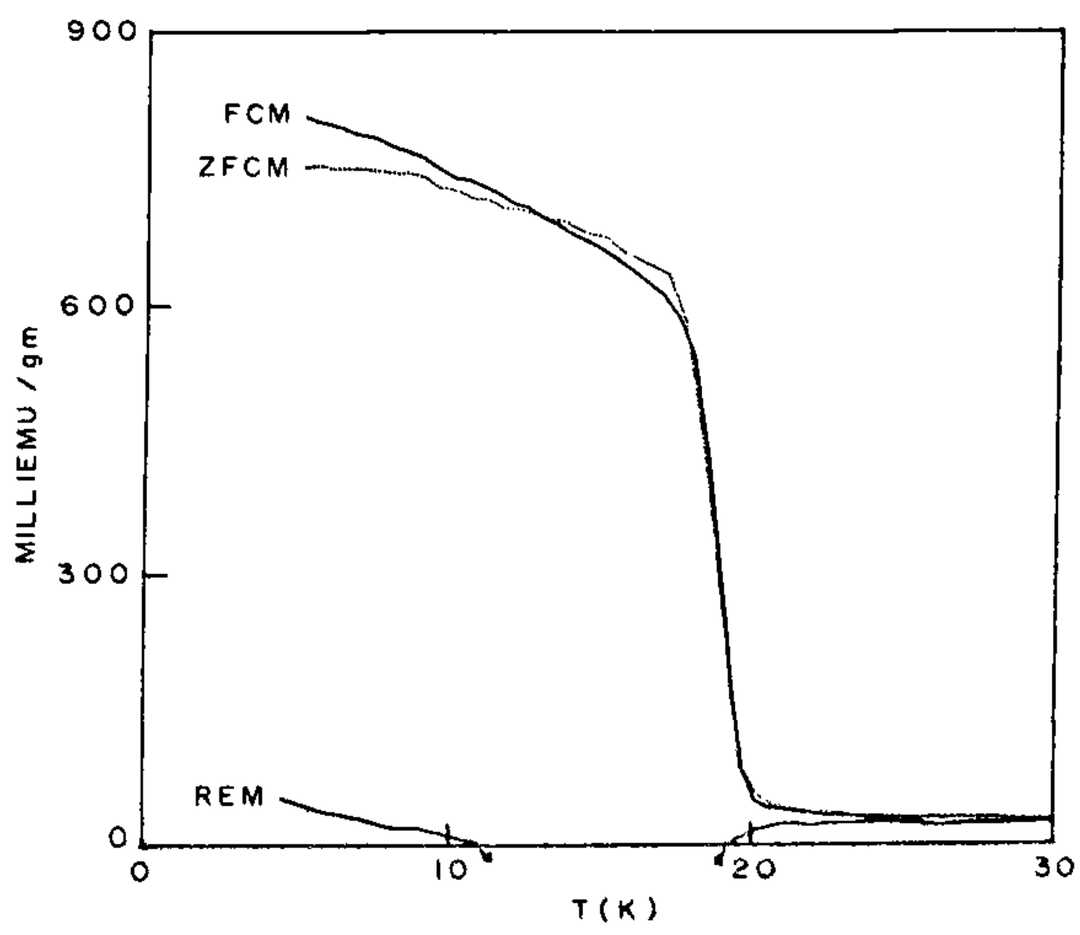


**Figure 1.** Zero field-cooled magnetization (ZFCM), field-cooled magnetization (FCM) and remanent magnetization (REM) data as a function of temperature for the sample **B**, i.e. $(NBu_4)_2Mn_2[Cu(opba)]_3$. The REM plot shows negative values between 11 K and 19 K, as indicated by small arrows.

applied fields, as shown in Figure 3 typically for 100 Oe and 500 Oe. The negative values of remanence, particularly, the valley-like feature has never been reported for molecular organic ferromagnets. In fact, generally, the value of Curie temperature is identified as the temperature where the value of REM falls exactly to zero. Magnitudes of REM may vary among different polycrystalline samples of a particular ferromagnet because it is generally recognized that it is influenced by sample-dependent factors such as the grain size and the shape. The valley-like feature in the REM plot indicates some kind of compensation behaviour between the two ferromagnetic sublattices, because the basic building blocks for our samples **A** and **B** are the ferrimagnetic $Mn_2^{II}Cu_3^{II}$ planar units[6].

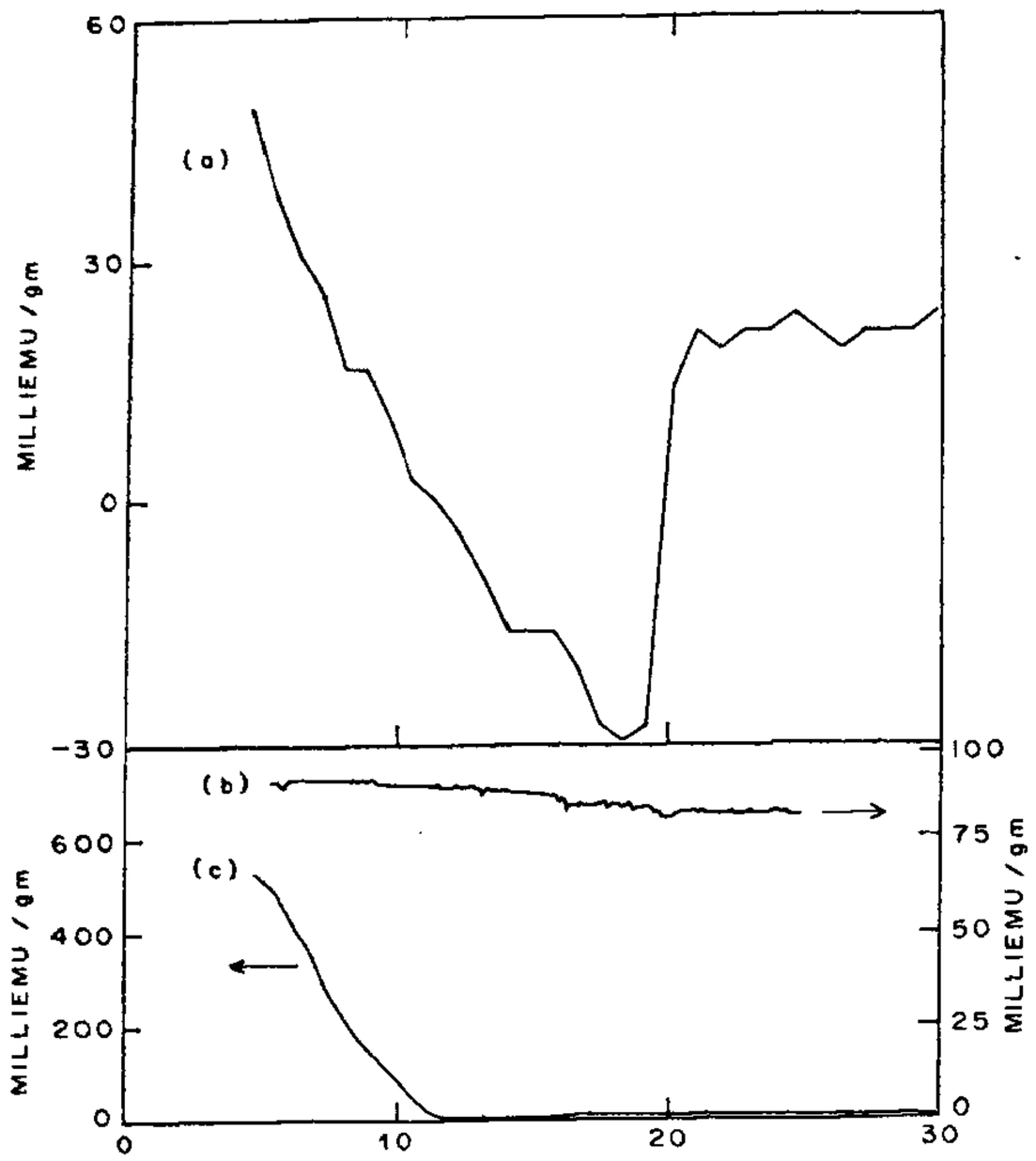


**Figure 2.** Remanent magnetization data for: (a) the sample **B**, i.e. $(NBu_4)_2Mn_2[Cu(opba)]_3$; (b) nickel standard; and (c) $MnCu(obbz) \cdot 1H_2O$. All these samples were cooled to 5 K in a field of 10 Oe before recording the data.

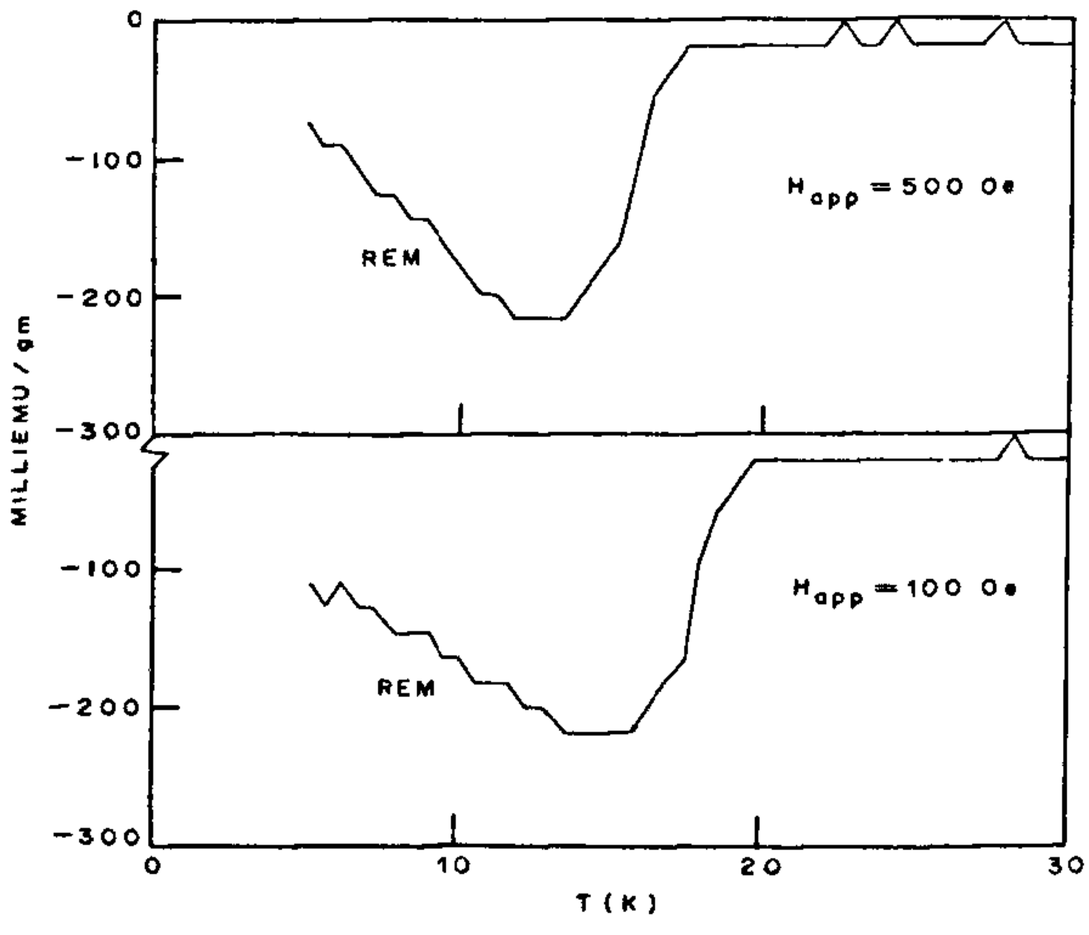


**Figure 3.** Remanent magnetization data for the sample **B** after it was cooled to 5 K in applied fields of 100 Oe and 500 Oe, respectively, before recording the data.

The *M* vs *H* plot for the sample **B** recorded at 5 K under the application of 500 Oe field is nearly an S-shaped curve with very little width or hysteresis (Figure 4). The low-field (−40 Oe to +40 Oe) portion of the *M* vs *H* plot exhibits a criss-crossing between the curves corresponding to increasing or decreasing field. The low-field portion of the *M* vs *H* plot for the same sample recorded at 5 K under the maximum applied field of 50 Oe is also shown in the inset of this figure.

The ZFCM and FCM magnetization plots for the sample **A** showed conventional behaviour with a hump below $T_c$ in the ZFCM as reported by Stumpf *et al.*[6], except that the magnitudes of ZFCM and FCM at 5 K were 80 and 285 memu/g in our case. The remanence for the sample **A**, too, showed negative values but no valley-like feature. The value of REM between 5 K and 13 K remained nearly constant (− 285 memu/g), becoming zero at ~ 16 K upon warming. The *M* vs *H* plot for the sample **A**, too, showed features exactly similar to those exhibited by the sample **B**. These observations indicate that the unusual magnetization behaviour is inherent in $(NBu_4)_2Mn_2[Cu(opba)]_3$ assembly. The only other report of an unusual magnetic behaviour for a molecular ferromagnet is the observation[8] of a strong negative magnetization below 30 K for $(NBu_4)Fe^{II}Fe^{III}(C_2O_4)_3$.

At this stage, the mechanism giving rise to the observation of negative remanence in our sample is not clear and is at best speculative. In general, a negative remanent magnetization could imply a field-induced mag-

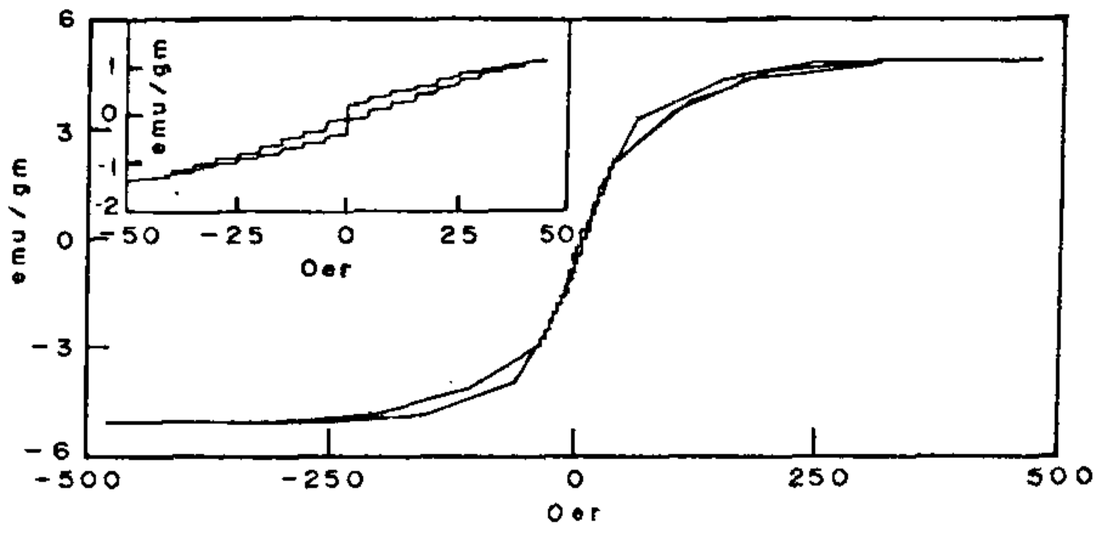


**Figure 4.** *M* vs *H* plots for the sample **B** recorded at 5 K under the application of 500 Oe (main figure) and 50 Oe (inset).

netization effect wherein a sample that is magnetic in the presence of a field, becomes diamagnetic in the absence of a field. However, these bimetallic organic magnets are known to exhibit spontaneous magnetization below $T_c$ even in the absence of an applied field. It is possible that a negative remanent magnetization arises in our samples **A** and **B** due to the antiferromagnetic coupling of hard and soft regions.

1. Miller, J. S., Calabrese, J. C., Bigelow, R. W., Epstein, A. J., Zhang, J. H. and Reiff, W. M., *J. Chem. Soc. Chem. Commun.*, 1986, 1026–1028.
2. Kahn, O., Pei, Y., Verdaguer, M., Renard, J. P. and Sletten, J., *J. Am. Chem. Soc.*, 1988, **110**, 782–789.
3. Nakatani, K., Bergerat, P., Codjovi, E., Mathoniere, C., Pei, Y. and Kahn, O., *Inorg. Chem.*, 1991, **30**, 3978–3980.
4. Nakatani, K., Carriat, J. Y., Journaux, Y., Kahn, O., Lloret, F., Renard, J. P., Pei, Y., Sletten, J. and Verdaguer, M., *J. Am. Chem. Soc.*, 1989, **111**, 5739–5748.
5. Stumpf, H. O., Pei, P., Mechaut, C., Kahn, O., Renard, J. P. and Ouahab, L., *Chem. Mat.*, 1994, **6**, 257–259.
6. Stumpf, H. O., Pei, Y., Kahn, O., Sletten, J. and Renard, J. P., *J. Am. Chem. Soc.*, 1993, **115**, 6738–6745.
7. Menvuk, N., Dwight, K. and Wickham, D. G., *Phys. Rev. Lett.*, 1960, **4**, 119–120.
8. Mathoniere, C., Carling, S. G., Sheng, D. Y. and Day, P., *J. Chem. Soc. Chem. Commun.*, 1994, 1551–1552.

Received 12 July 1995; revised accepted 17 November 1995

# Candidate live oral cholera vaccine strains produce a new cholera toxin

**D. V. Singh, Anjali Tikoo and S. C. Sanyal**

Department of Microbiology, Institute of Medical Sciences, Banaras Hindu University, Varanasi 221 005, India

**When six candidate live oral cholera vaccine strains deleted for one or all known virulence factors are tested for enterotoxin production, two of them caused fluid accumulation in the initial rabbit ileal loop (RIL) test, the others did so after 1–3 serial passages through RIL. Culture filtrates also showed similar secretory response. Ten times concentrated culture filtrates of these strains gave precipitin band against anti-new cholera toxin showing reaction of identity. These observations clearly indicate that vaccine strains produce a secretogen antigenically similar to the new cholera toxin.**

STRAINS of *Vibrio cholerae* 01 have been reported to secrete a number of extracellular products, such as haemolysin (Hly), zonula occludens toxin (Zot), accessory cholera enterotoxin (Ace) including the well-known cholera toxin (CT)[1]. Although CT has been suggested to be the factor responsible for severe cholera, however, if its gene is deleted the other toxic factors when present in some strains have been demonstrated to cause a mild secretory response[1]. However, it was evident from a recent volunteer study using a Tox-mutant of the biotype El Tor 01 Ogawa strain E 7946 designated CVD 110 that was deleted of all the above toxic factors, was still capable of causing diarrhoea in seven of ten volunteers[2]. These observations clearly indicate that such strains produce another secretogen.

It was shown earlier that CT gene-negative and positive strains of *V. cholerae* 01, biotype classical or El Tor, serotype Ogawa or Inaba of clinical or environmental origin or genetically engineered in the laboratory, produce a new cholera toxin (NCT) and the disease cholera can be caused by either CT or NCT or both[3,4]. An attempt was, therefore, made in this study to examine if the candidate vaccine strains of *V. cholerae* (obtained from J. B. Kaper, CVD, Maryland) deleted for one or all the other toxic factors produce NCT (Table 1).

Live cells of two of the six candidate vaccine strains tested in ligated ileal loops of adult albino rabbits (Belgian strain) following the method of De and Chatterjee[5], caused fluid accumulation in the initial tests, the others did so after 1–3 consecutive passage/s through RILs (Table 2), and thereafter outpouring of fluid by every strain increased on each passage (data not shown).

Culture filtrates of all the strains also caused fluid accumulation, although slightly less than that of the

**Table 1.** Virulence patterns of candidate vaccine strains

| Vaccine strain | Parent strain | Virulence patterns | | | | |
|---|---|---|---|---|---|---|
| | | CTA | CTB | Hly | Zot | Ace |
| JBK 70 | El Tor N 16961 | – | – | + | + | + |
| CVD 104 | El Tor N 16961 | – | – | – | + | + |
| CVD 101 | Classical 395 | – | + | + | + | + |
| CVD 105 | Classical 395 | – | + | – | + | + |
| CVD 109 | El Tor 7946 | – | – | + | – | – |
| CVD 110 | El Tor 7946 | – | + | – | – | – |

**Table 2.** Enterotoxicity of the genetically engineered vaccine strains

| Vaccine strain | Range of fluid accumulations (ml/cm of RIL*) | | Number of passages |
|---|---|---|---|
| | Live cells | Culture filtrates | |
| JBK 70 | 0.58–1.00 | 0.54–1.2 | 0 |
| CVD 104 | 0.60–1.10 | 0.56–1.1 | 2 |
| CVD 101 | 0.60–1.20 | 0.50–1.0 | 3 |
| CVD 105 | 0.50–0.90 | 0.53–1.2 | 1 |
| CVD 109 | 0.71–0.98 | 0.66–1.0 | 0 |
| CVD 110 | 0.66–0.84 | 0.60–0.9 | 3 |
| Positive control† | 0.80–1.50 | 0.92–1.4 | 0 |
| Negative control‡ | 0.0 | 0.0 | – |

*Range of accumulated fluid in ileal loops of two rabbits.
†BHIB culture of toxigenic strain 569B of *V. cholerae* 01.
‡BHIB.